

Supplementary Information:
Mechanism for reconfigurable logic in disordered dopant networks

Henri Tertilt¹, Jesse Bakker², Marlon Becker¹, Bram de Wilde², Indrek Klanberg²,

Bernard J. Geurts^{3,4}, Wilfred G. van der Wiel^{2,5}, Andreas Heuer¹, Peter A. Bobbert^{2,6}

¹*Institut für physikalische Chemie, Westfälische Wilhelms-Universität Münster, Münster, Germany*

²*NanoElectronics Group, MESA+ Institute for Nanotechnology,*

and Center for Brain-Inspired Nano Systems (BRAINS),

University of Twente, Enschede, The Netherlands

³*Multiscale Modeling and Simulation Group, Faculty of Electrical Engineering,*

Mathematics and Computer Science, and Center for Brain-Inspired Nano Systems,

University of Twente, Enschede, The Netherlands

⁴*Center for Computational Energy Research (CCER),*

Eindhoven University of Technology, 5600 MB Eindhoven, The Netherlands

⁵*Fachbereich Physik, Westfälische Wilhelms-Universität Münster, Münster, Germany*

⁶*Molecular Materials and Nanosystems Group and Center for Computational Energy Research,*

Eindhoven University of Technology, Eindhoven, The Netherlands

(Dated: August 9, 2021)

CONTENTS

S1. Influence of number of counterdopants	2
S2. Artificial evolution of Boolean logic in a second device	3
S3. Boolean logic with shorter simulation time	4
S4. Voltage and current distributions for random control voltages	5
S5. Voltage and current distributions for Boolean gates in a second device	6
S6. Correlations in output current for different logic inputs	7
S7. Sensitivity of AND and XOR gates to V_{c2} and V_{c3}	8
S8. Gate abundances in a second device	9
References	9

S1. INFLUENCE OF NUMBER OF COUNTERDOPANTS

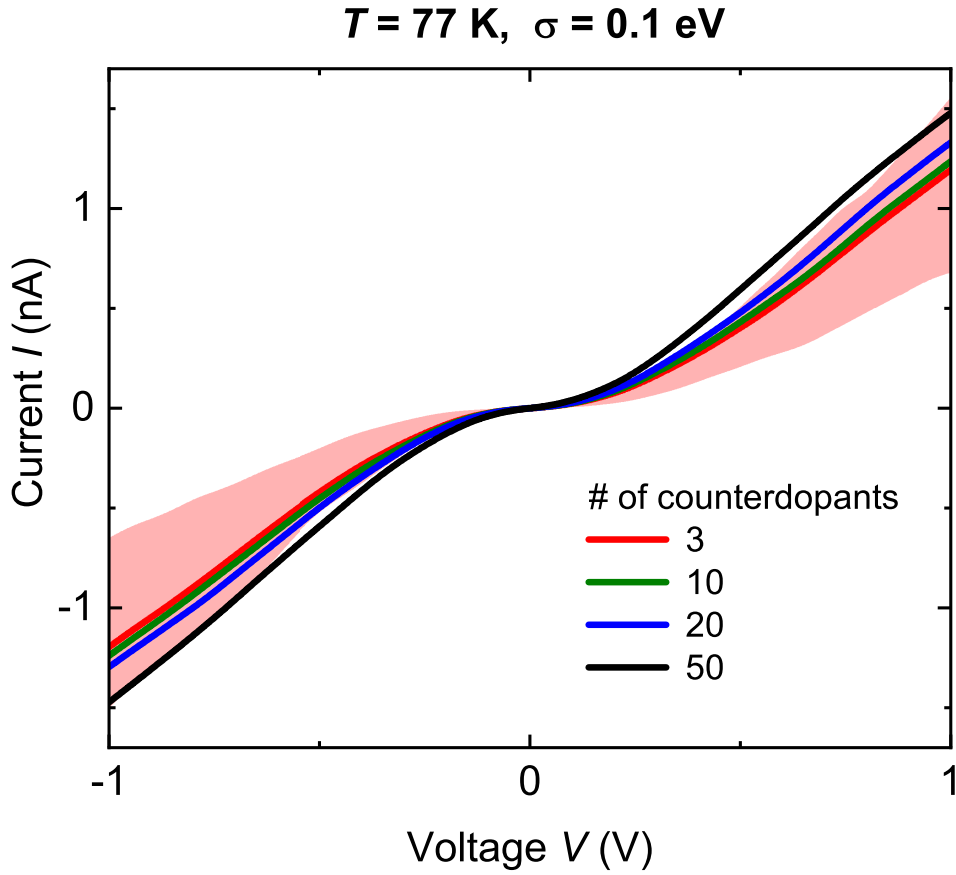


Figure S1. Simulated I - V characteristics at 77 K and energy disorder strength $\sigma = 0.1$ eV, averaged over the 8 neighbouring electrode combinations of 30 devices with different numbers of counterdopants. The result for 3 counterdopants is the same as in Fig. 1a of the main text, where half of the 240 I - V characteristics fall in the shaded red region. The averaged I - V characteristic for 50 counterdopants (black line) still falls in this region.

S2. ARTIFICIAL EVOLUTION OF BOOLEAN LOGIC IN A SECOND DEVICE

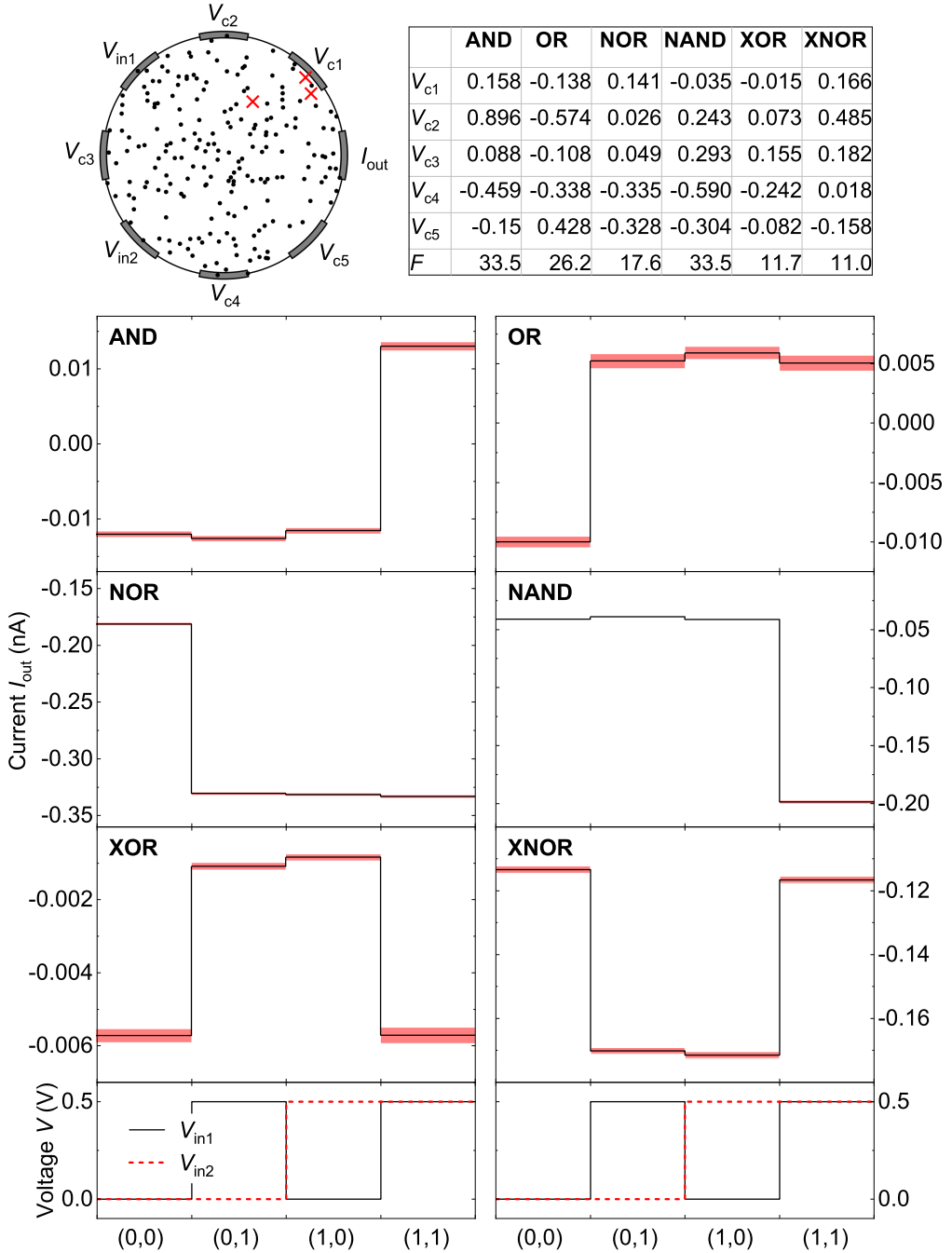


Figure S2. Boolean functionality at 77 K as found by artificial evolution in the device shown at the top left, which is different from that in Fig. 2 of the main text. The control voltages $V_{\text{c}1}$ – $V_{\text{c}5}$ and fitnesses F are given in the table at the top right.

S3. BOOLEAN LOGIC WITH SHORTER SIMULATION TIME

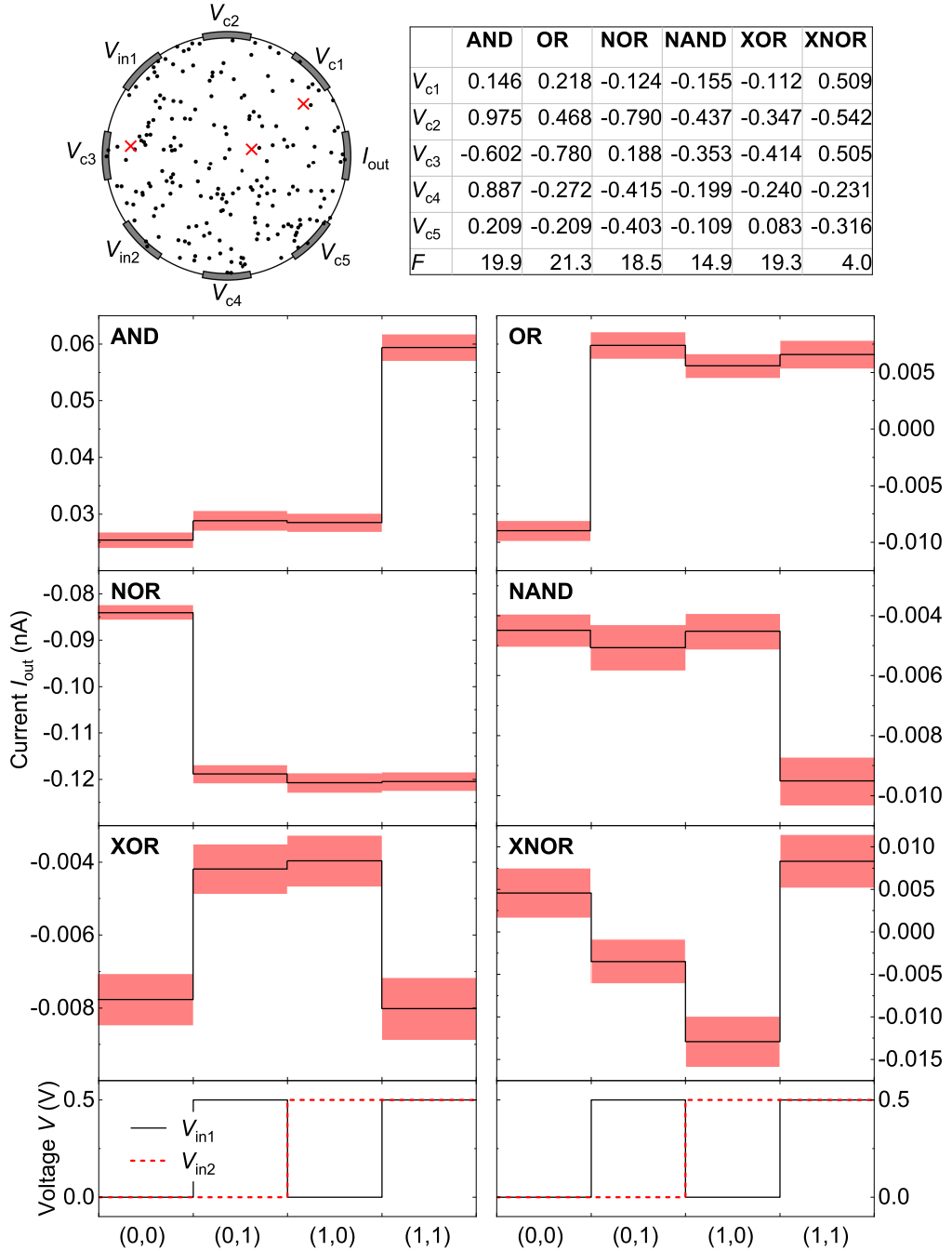


Figure S3. Same as in Fig. 2 of the main text, but with currents and uncertainties determined for 10^6 instead of 10^7 KMC steps. The control voltages V_{c1} – V_{c5} are unchanged.

S4. VOLTAGE AND CURRENT DISTRIBUTIONS FOR RANDOM CONTROL VOLTAGES

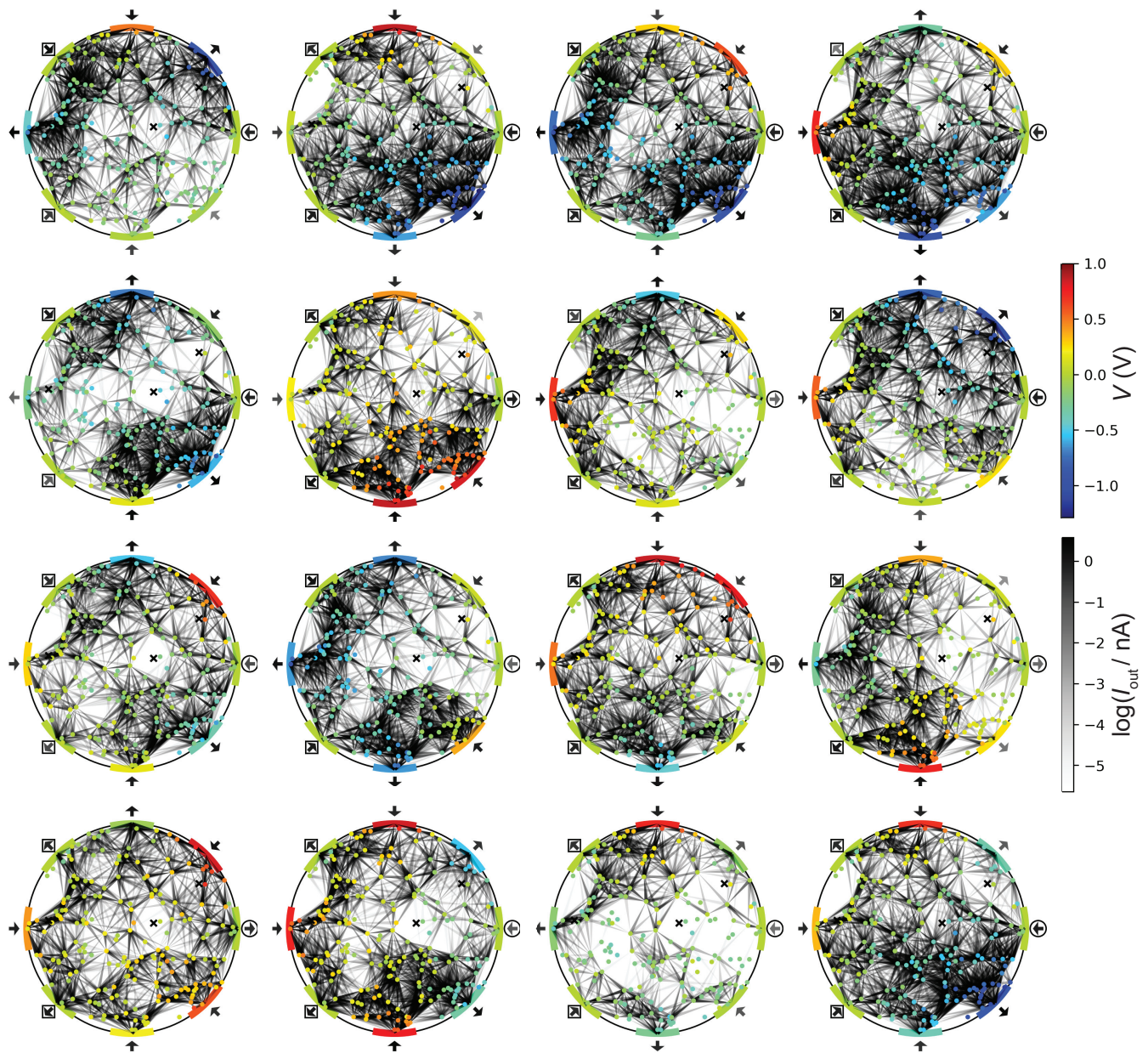


Figure S4. Voltages and currents for the device of Fig. 2 in the main text with 16 random control voltages in the interval $[-1,1]$ V and $(0,0)$ input.

S5. VOLTAGE AND CURRENT DISTRIBUTIONS FOR BOOLEAN GATES IN A SECOND DEVICE

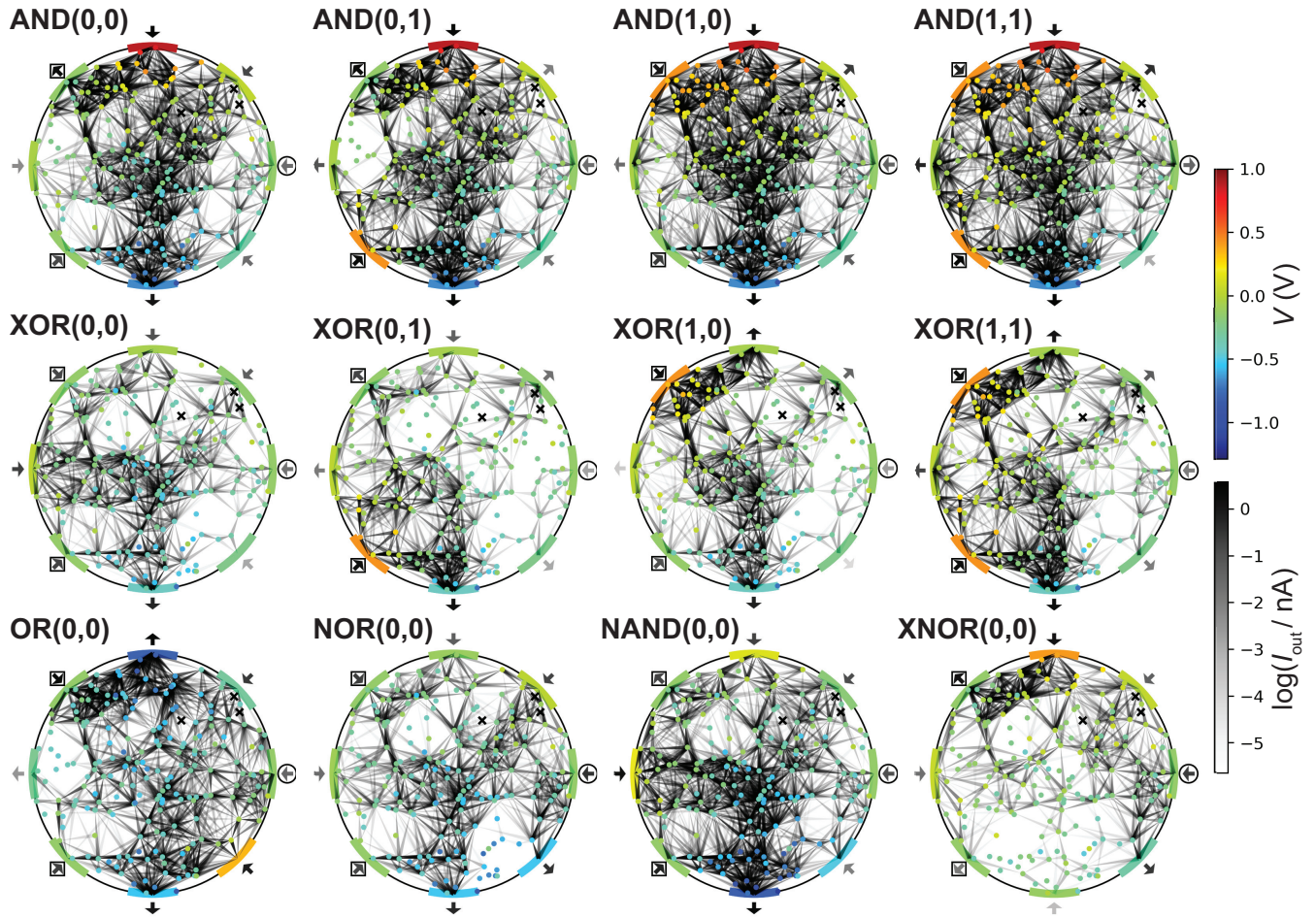


Figure S5. Voltages and currents for the device of Fig. S2. First row: AND gate for the four logic input combinations. Second row: XOR gate. Third row: OR, NOR, NAND, and XNOR gate with (0,0) input.

S6. CORRELATIONS IN OUTPUT CURRENT FOR DIFFERENT LOGIC INPUTS

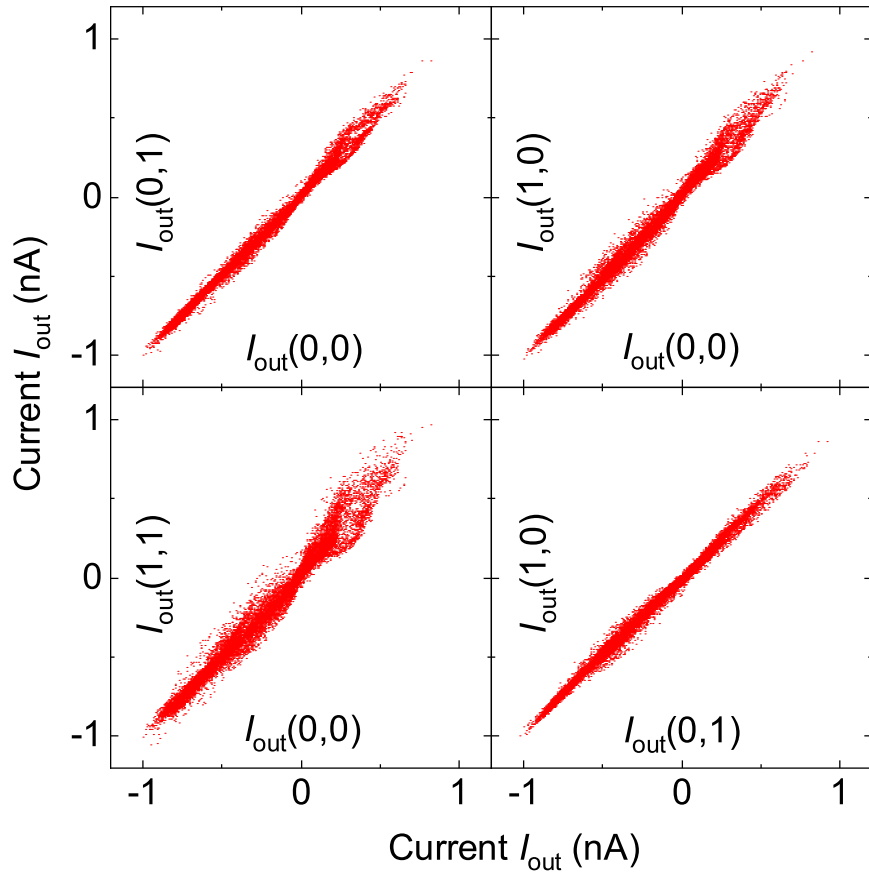


Figure S6. Correlations between current outputs of the device of Fig. 2 in the main text for logic inputs (0,0), (1,0), (0,1), and (1,1), and about 20,000 random combinations of the control voltages V_{c1} – V_{c5} in the interval [−1,1] V.

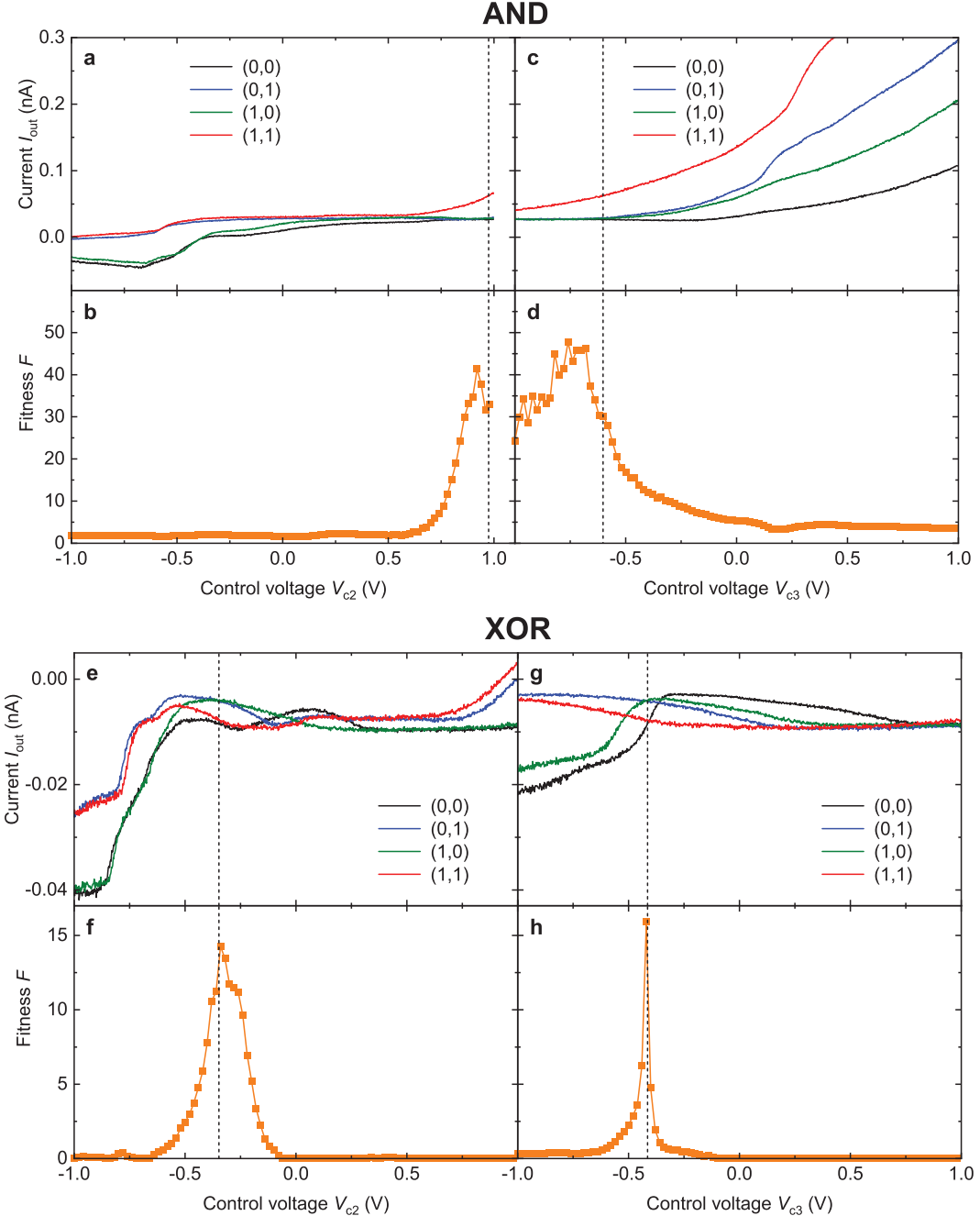
S7. SENSITIVITY OF AND AND XOR GATES TO V_{c2} AND V_{c3}


Figure S7. **a**, Output currents I_{out} for the four logic input combinations and **b** fitness F of the AND gate of Fig. 2 in the main text as a function of control voltage V_{c2} . Vertical dashed lines in a and b: value of V_{c2} found by artificial evolution. **c** and **d**, Same as a and b, but for V_{c3} . The evolutionary algorithm did not find before stopping the somewhat higher fitnesses of F in b and d at other values of V_{c2} and V_{c3} . **e–h**, Same as a–d, but for the XOR gate.

S8. GATE ABUNDANCES IN A SECOND DEVICE

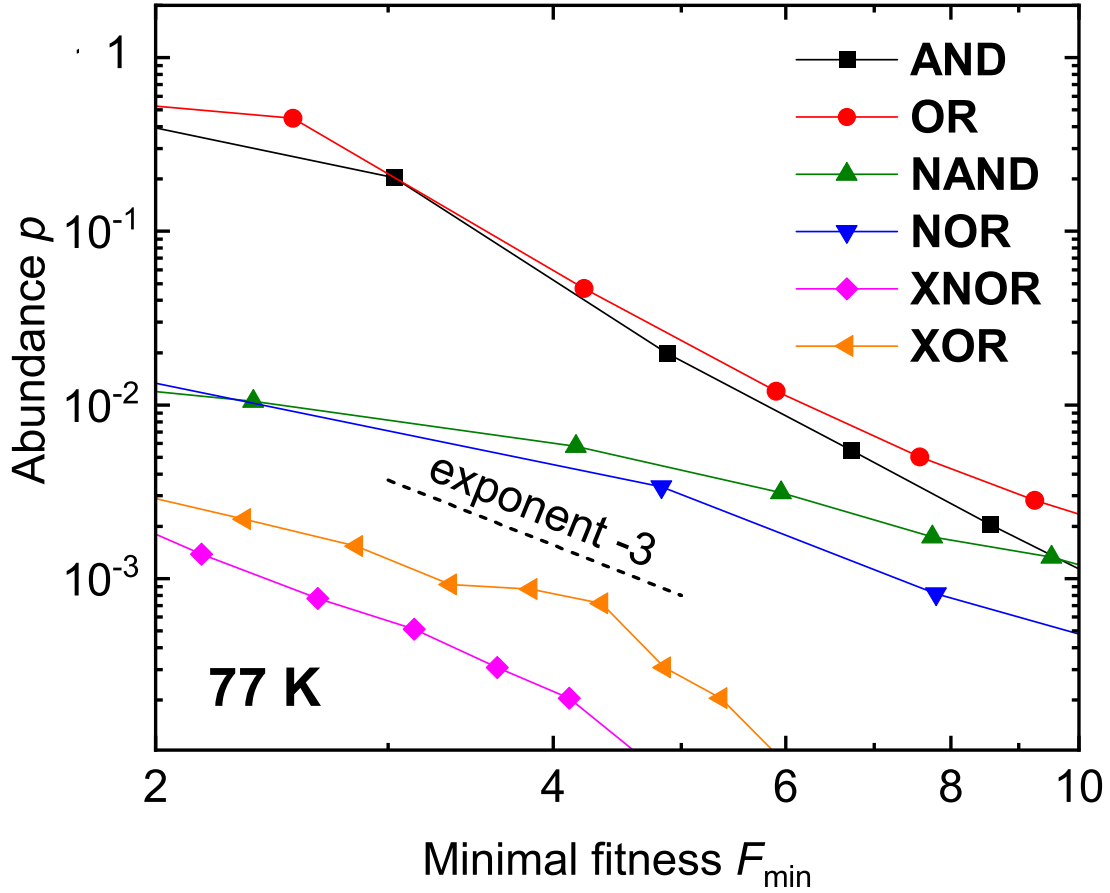


Figure S8. Abundance p of the six basic Boolean gates with minimal fitness F_{\min} among about 20,000 random combinations of the control voltages V_{c1} – V_{c5} of the device in Fig. S2 at 77 K. Fitnesses were obtained from simulations of 10^7 KMC steps for each combination. Dashed line: power law with exponent -3 .